

## The Carbon Dioxide–Water Interface at Conditions of Gas Hydrate Formation

Felix Lehmkuhler,<sup>\*,†</sup> Michael Paulus,<sup>†</sup> Christian Sternemann,<sup>†</sup> Daniela Lietz,<sup>†</sup>  
Federica Venturini,<sup>‡</sup> Christian Gutt,<sup>§</sup> and Metin Tolan<sup>†</sup>

*Fakultät Physik/DELTA, Technische Universität Dortmund, Maria-Goeppert-Mayer-Strasse 2, 44221 Dortmund, Germany, ESRF, BP 220, 38043 Grenoble, France, and HAYSLAB at DESY, Notkestrasse 85, 22607 Hamburg, Germany*

Received August 7, 2008; E-mail: Felix.Lehmkuehler@tu-dortmund.de

**Abstract:** The structure of the carbon dioxide–water interface was analyzed by X-ray diffraction and reflectivity at temperature and pressure conditions which allow the formation of gas hydrate. The water–gaseous CO<sub>2</sub> and the water–liquid CO<sub>2</sub> interface were examined. The two interfaces show a very different behavior with respect to the formation of gas hydrate. While the liquid–gas interface exhibits the formation of thin liquid CO<sub>2</sub> layers on the water surface, the formation of small clusters of gas hydrate was observed at the liquid–liquid interface. The data obtained from both interfaces points to a gas hydrate formation process which may be explained by the so-called local structuring hypothesis.

### Introduction

Beyond the three classical states of matter, water can form an additional solid phase called clathrate hydrate with the auxiliary presence of gas molecules, typically at low temperatures and high pressures.<sup>1,2</sup> In these crystalline structures the gas molecules are trapped in a hydrogen bond water cage network. During the past years, hydrates have become very important materials since they may become essential for future energy recovery or hydrogen and CO<sub>2</sub> storage.<sup>2–6</sup>

The hydrate formation process is well understood from a macroscopic thermodynamical point of view.<sup>7</sup> Nevertheless, the formation on a microscopic level is still not clear. In the literature, three competing formation models are presented. Within the framework of the cluster nucleation theory by Sloan,<sup>1</sup> gas molecules dissolve in water, and labile clusters are formed and agglomerate, preferentially next to the water surface. After a critical cluster size is achieved, the macroscopic nucleation sets in. A different model resulting from molecular dynamics (MD) simulations of the water–liquid CO<sub>2</sub> interface is the local structuring hypothesis.<sup>8</sup> Here the water and gas molecules arrange stochastically until an arrangement similar to the hydrate phase is reached. This stochastically achieved network is

stabilized after exceeding a certain size and hydrate crystals start growing. In the third model introduced by Rodger<sup>9</sup> a surface-driven formation is proposed. Gas molecules adsorb on the water surface and are trapped in the center of partially completed water cavities. Kvamme<sup>10,11</sup> extended this model based on results of MD simulations and predicted the initial nucleation at the water–CO<sub>2</sub> interface. Due to wave motion of the water surface the mixing of water and gas molecules is supported, and hydrate fragments can be formed. The cluster nucleation theory and the surface-driven model predict the appearance of hydrate prestages at the water surface. In contrast, the local structuring hypothesis predicts a spontaneous formation without any precursor clusters. A comparison of the local structuring hypothesis and the cluster nucleation theory is presented in Figure 1. Due to their similarity, cluster nucleation theory and surface-driven model are merged. The contrast between presence and absence of prehydrate structures is clearly visible.

Several MD-simulations which have been performed during the past years have not been able to prove one of these theories explicitly. Some of the simulations support the local structuring hypothesis<sup>12–14</sup> while others find a labile cluster formation,<sup>15,16</sup> or at least an indication of hydrate precursor.<sup>17</sup> It is the aim of this paper to solve this question from the experimental point of view.

<sup>†</sup> Technische Universität Dortmund.

<sup>‡</sup> ESRF, Grenoble.

<sup>§</sup> HAYSLAB, Hamburg.

- (1) Sloan, E. D.; Koh, C. A. *Clathrate Hydrates of Natural Gases*; CRC Press Inc.: Boca Ranton, 2007.
- (2) Sloan, E. D. *Nature* **2003**, *426*, 353–359.
- (3) Florusse, L. J.; Peters, C. J.; Schoonman, J.; Hester, K. C.; Koh, C. A.; Dec, S. F.; Marsh, K. N.; Sloan, E. D. *Science* **2004**, *306*, 469–471.
- (4) Lee, H.; Lee, J.; Kim, D. Y.; Park, J.; Seo, Y.; Zeng, H.; Moudrakovski, I. L.; Ratcliffe, C. I.; Ripmeester, J. A. *Nature* **2005**, *434*, 743–746.
- (5) Brewer, P. G.; Friederich, G.; Peltzer, E. T.; Orr, F. M., Jr. *Science* **1999**, *284*, 943–945.
- (6) Kang, S. P.; Lee, H. *Environ. Sci. Technol.* **2000**, *34*, 4397–4400.
- (7) van der Waals, J. H.; Platteeuw, J. C. *Adv. Chem. Phys.* **1959**, *2*, 1–57.
- (8) Radhakrishnan, R.; Trout, B. L. *J. Chem. Phys.* **2002**, *117*, 1786–1796.

(9) Rodger, P. M. *J. Phys. Chem.* **1990**, *94*, 6080–6089.

(10) Kvamme, B. *Ann. N.Y. Acad. Sci.* **2000**, *912*, 496–501.

(11) Kvamme, B. Initiation and growth of hydrate from nucleation theory; *Proceedings of the International Symposium on Deep Sea Sequestration of CO<sub>2</sub>*, 2000, 1-1-1.

(12) Hirai, S.; Okazaki, K.; Tabe, Y.; Kawamura, K. *Energy Convers. Manage.* **1997**, *38*, S301–S306.

(13) Moon, C.; Taylor, P. C.; Rodger, P. M. *J. Am. Chem. Soc.* **2003**, *125*, 4706–4707.

(14) Guo, G. J.; Zhang, Y. G.; Liu, H. *J. Phys. Chem. C* **2007**, *111*, 2595–2606.

(15) Long, J.; Sloan, E. D. *Mol. Simul.* **1993**, *11*, 145–161.

(16) Guo, G. J.; Zhang, Y. G.; Zhao, Y. J.; Refson, K.; Shan, G. H. *J. Chem. Phys.* **2004**, *121*, 1542–1547.

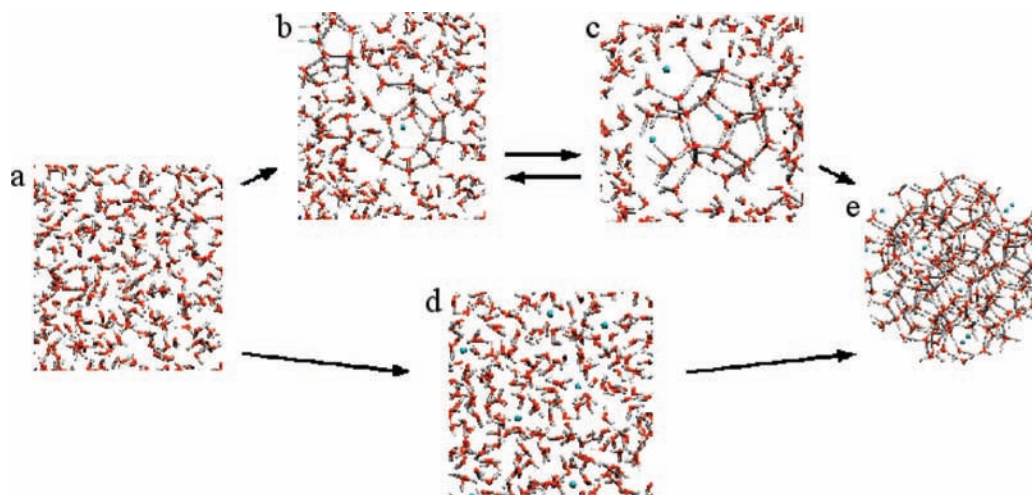


**Figure 1.** Comparison of the cluster nucleation theory (a-b-c-e) and the local structuring hypothesis (a-d-e). (a) Water without dissolved gas molecules (initial condition). (b) Cluster form immediately after dissolution of gas molecules. (c) Cluster prestages agglomerate by sharing faces. These agglomerated clusters may be unstable (step back to b is possible). (d) No cluster formation after dissolution of gas molecules. (e) Hydrate nucleation.

A lot of experimental attempts to study the hydrate formation process have been performed in the past. Within most of these studies the hydrate formation is observed as an interfacial phenomenon. However, the methods used, such as optical observation or calorimetric measurements, only give information about the formation after the initial nucleation has already taken place. Takeya et al. reported a formation on a macroscopic level at a liquid–liquid interface where the initial nucleation starts at the water surface.<sup>18</sup> According to this study, needle-like hydrate clusters grow toward the water bulk. The hydrate formation from water and gaseous CO<sub>2</sub> was reported by Morgan and co-workers who observed the growing hydrate crystals optically and by means of calorimetric methods.<sup>19</sup> Here, the gaseous CO<sub>2</sub> was bubbled through the water bulk for several minutes to induce the hydrate formation. A different approach has been followed by Ohmura et al.<sup>20</sup> In order to observe methane hydrate formation the authors used water spraying and, by optical observation, found a hydrate formation that starts at the water surface. As stated before, neither hydrate prestructure formation nor the initial nucleation can be observed with the use of these methods. Koh and co-workers showed time-resolved macroscopic hydrate formation in the stirred water–CO<sub>2</sub> bulk mixture by means of X-ray diffraction.<sup>21</sup> The authors were not able to favor one hydrate formation model due to measurements of a disturbed system which offers seeds for macroscopic hydrate formation, but they proposed a dynamic intermediate phase during the hydrate formation and growth process. In general, the quantity measured in all of these experiments is the induction time  $t_i$  for hydrate nucleation. This induction time depends on the kind of guest molecules, the degree of supercooling, and the history of the water–gas system.<sup>1,18</sup> For CO<sub>2</sub> the induction time is on the order of  $t_i \approx 2h$ . Thus, so far there are no data regarding the gas hydrate formation process

at nanometer length scales for the early state before the macroscopic formation begins. In this work the first study of the CO<sub>2</sub>–water interface on molecular length scales is presented.

## Experiment and Discussion

**Liquid–Gas Interface.** The prestage formation at or near the surface predicted by the cluster nucleation theory and the surface-driven model will cause an increased surface roughness and the appearance of layers of incomplete hydrate cages at the surface. These changes in surface roughness and the formation of thin layers are observable by X-ray reflectivity measurements.

X-ray reflectivity is a powerful tool to investigate the formation of very thin layers on solid and liquid surfaces with ångstrom resolution.<sup>22</sup> Its great advantage compared to other methods is the possibility to identify in situ surface roughness changes of molecular thin films from the reflectivity measurements. In such experiments the wave vector transfer has only one component perpendicular to the surface given by

$$q_z = (4\pi/\lambda) \sin(\theta)$$

where  $\theta$  denotes the angle between the sample surface and the X-ray beam, and  $\lambda$  the wavelength of the incident beam.

The scattered intensity  $R$  is given by<sup>22,23</sup>

$$R(q_z) = R_F(q_z) \cdot \left| \frac{1}{\rho_\infty} \int \frac{d\rho_e(z)}{dz} e^{iq_z z} dz \right|^2 \quad (1)$$

with  $R_F$  the Fresnel reflectivity of a smooth surface and  $\rho_\infty$  the average density of the entire sample. Thus, X-ray reflectivity yields the laterally averaged density profile perpendicular to the sample's surface.

Pressure-dependent X-ray reflectivity measurements of the water–CO<sub>2</sub> interface were performed at the European Synchrotron Radiation Facility (ESRF) using the high-energy setup for liquid surfaces at beamline ID15A.<sup>24,25</sup> CO<sub>2</sub> and water form the cubic structure I (sI) hydrate with a lattice constant of 12 Å.<sup>2</sup> At  $T = 0^\circ\text{C}$  a minimum pressure of  $p = 12.5$  bar is

(17) Zhang, J.; Hawtin, R. W.; Yang, Y.; Nakagawa, E.; Rivero, M.; Choi, S. K.; Rodger, P. M. *J. Phys. Chem. B* **2008**, *112*, 10608–10618.

(18) Takeya, S.; Hori, A.; Hondoh, T.; Uchida, T. *J. Phys. Chem. B* **2000**, *104*, 4164–4168.

(19) Morgan, J. J.; Blackwell, V. R.; Johnson, D. E.; Spencer, D. F.; North, W. J. *Environ. Sci. Technol.* **1999**, *33*, 1448–1452.

(20) Ohmura, R.; Kashiwazaki, S.; Shiota, S.; Tsuji, H.; Mori, Y. H. *Energy Fuels* **2002**, *16*, 1141–1147.

(21) Koh, C. A.; Savidge, J. L.; Tang, C. C. *J. Phys. Chem.* **1996**, *100*, 6412–6414.

(22) Tolan, M. *X-ray Scattering from Soft Matter Thin Film*; Springer: Berlin, 1999.

(23) Als-Nielsen, J.; McMorrow, D. *Elements of Modern X-Ray Physics*; John Wiley & Sons: New York, 2001.

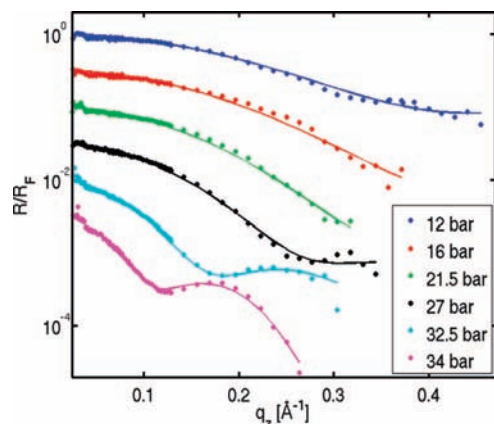


**Figure 2.** Reflectivities normalized by the Fresnel reflectivity for selected CO<sub>2</sub> pressures. Solid lines represent fits. The curves are shifted for clarity.

necessary for a stable CO<sub>2</sub> hydrate structure.<sup>1</sup> Ultrapure water filtered by a Millipore apparatus, and CO<sub>2</sub> purchased from Air Liquide with a purity of 99.998% was employed. The photon energy was  $E = 72.5$  keV. A pressure cell with aluminum windows was utilized to measure at gas pressures up to 35 bar. The temperature was chosen to be 0.15 °C, therefore avoiding the formation of ice and controlled with an accuracy of 0.01 °C. A few mm thick water film was prepared in the sample cell, forming a well-defined meniscus. CO<sub>2</sub> was allowed to fill the cell via an inlet. Following each reflectivity measurement, the detector was moved to an out-of-plane position in order to measure the diffusely scattered intensity that is necessary for an accurate background subtraction. Measurements for different gas pressures between 1 bar and the condensation pressure of 35 bar were carried out. For pressures above 33 bar the time dependence of the reflectivity curves was investigated. For a given pressure, this was done by performing several measurements within a time interval of more than 8 h. During this period the sample was not stirred or disturbed in other ways to favor hydrate formation. Thus, it should be possible to detect hydrate prestructures without offering nucleation seeds. Also surface-sensitive diffraction measurements were performed to detect Bragg reflections originating from possible CO<sub>2</sub> hydrate crystallites.

Reflectivities for different gas pressures are presented in Figure 2. The oscillations indicate the formation of thin layers on the water surface. The curves are fitted using the effective density model<sup>22</sup> based on Parratt's algorithm.<sup>26</sup> Refined electron density profiles are presented in Figure 3. The measurement at 1 bar CO<sub>2</sub> pressure yields a roughness of the water surface of  $\sigma = (3.2 \pm 0.1)$  Å, which is in good agreement with capillary wave theory.<sup>27</sup> The measured water roughness does not change with increasing gas pressure. Most importantly, this is also the case when the pressure range where gas hydrate formation becomes possible was reached. An electron density of  $\rho_L = (0.282 \pm 0.008)$  e/Å<sup>3</sup> was found for the observed layers and fits very well with the tabulated value  $\rho_{\text{CO}_2} = 0.279$  e/Å<sup>3</sup> for liquid CO<sub>2</sub>. This suggests the adsorption of gas molecules instead of hydrate formation because the electron density of

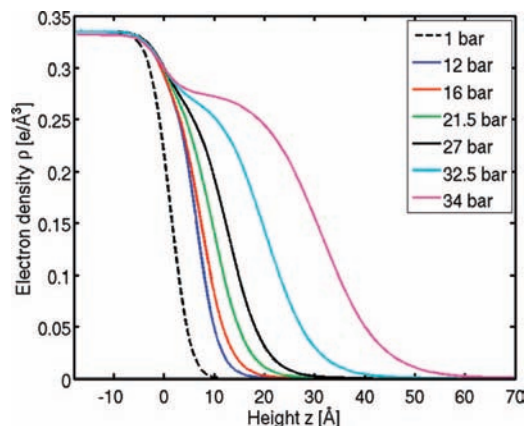


**Figure 3.** Electron density profiles corresponding to the refinements of Figure 2 for different gas pressures.

CO<sub>2</sub> hydrate is approximately 30% higher compared to that of liquid CO<sub>2</sub>.<sup>28</sup> The roughness of this CO<sub>2</sub> layer ranges from 3 Å at low gas pressures to 11 Å at pressures near the condensation pressure. In order to explain the data, capillary wave and adsorption theory can be applied. The adsorption of gas molecules on the liquid surface as a function of gas pressure is a result of van der Waals interactions between the liquid and the vapor phase. It is usually described by an adsorption isotherm in the framework of the Frenkel–Halsey–Hill (FHH) theory.<sup>29</sup> The thickness  $l_m$  of the adsorbed layer can be calculated via the free energy  $F$  of the liquid–gas system yielding<sup>29</sup>

$$l_m = \left( \frac{A_{\text{eff}}}{6\pi\Delta\rho k_B T \ln(p/p_0)} \right)^{\frac{1}{3}} \quad (2)$$

Here,  $A_{\text{eff}}$  denotes the effective Hamaker constant,  $\Delta\rho$  is the density difference between the adsorbed layer and the gas phase, and  $p_0$  is the condensation pressure of the gas at the fixed temperature  $T$ .

An adsorption isotherm can be fitted to the layer thickness determined from the measured data. A good agreement between experiment and calculation is achieved (see Figure 4). This suggests again the absence of gas hydrate structures. Besides, the inset in Figure 4 shows the layer roughness as a function of layer thickness. The agreement of experimental results and theory for adsorbed liquid films<sup>29</sup> is again very good. Owing to the good interpretation of the data, only the formation of adsorbed liquid CO<sub>2</sub> layers can be observed, but no indication of hydrate or hydrate prestage formation after more than 8 h was found. This is in qualitative agreement with measurements at the water–propane interface.<sup>30</sup> Furthermore, no Bragg reflections could be observed by X-ray diffraction at this interface. Therefore, the formation of hydrate crystallites must be very weak – if there is any.

**Liquid–Liquid Interface.** As no hydrate formation at the water–gaseous CO<sub>2</sub> interface was visible, the pressure was raised to a value above the condensation pressure of CO<sub>2</sub>. Thus, a macroscopic liquid CO<sub>2</sub> layer with a thickness of several millimeters is formed at the water surface. In order to observe

(24) Reichert, H.; Honkimäki, V.; Snigirev, A.; Engemann, S.; Dosch, H. *Physica B* **2003**, *336*, 46–55.

(25) Honkimäki, V.; Reichert, H.; Okasinski, J. S.; Dosch, H. *J. Synchrotron Radiat.* **2006**, *13*, 426–431.

(26) Parratt, L. G. *Phys. Rev. Lett.* **1954**, *95*, 359–369.

(27) Braslau, A.; Pershan, P. S.; Swislow, G.; Ocko, B. M.; Als-Nielsen, J. *Phys. Rev. A* **1988**, *38*, 2457–2470.

(28) Uchida, T.; Ebinuma, T.; Narita, H. Laboratory studies on the formation and dissociation processes of CO<sub>2</sub>-hydrate crystals; *Proceedings of the International Symposium on Deep Sea Sequestration of CO<sub>2</sub>*, 2000, 1–4-1.

(29) Paulus, M.; Gutt, C.; Tolan, M. *Phys. Rev. E* **2005**, *72*, 061601.

(30) Paulus, M.; Gutt, C.; Tolan, M. *Surf. Interface Anal.* **2008**, *40*, 1226–1230.



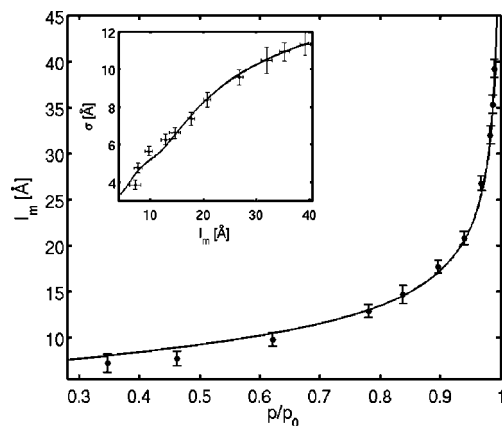


**Figure 4.** Adsorption isotherm, solid line represents the fitted curve,  $p_0 = 34.99$  bar.<sup>31</sup> (Inset) Surface roughness of the adsorbed CO<sub>2</sub> layer as function of layer thickness. Solid line represents a calculation within the so-called *anharmonic approximation*.<sup>29</sup>

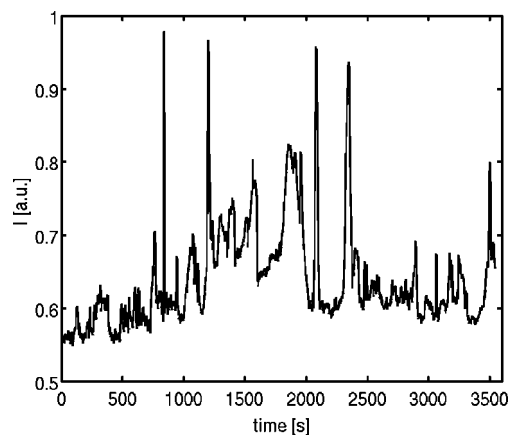


**Figure 5.** Timescan of the (321) Bragg reflection of CO<sub>2</sub> hydrate measured at the water–liquid CO<sub>2</sub> interface.

the formation of gas hydrate, X-ray diffraction measurements were performed at this liquid–liquid interface. The studied interface area was about 1 mm<sup>2</sup>. Bragg reflections of CO<sub>2</sub> hydrate were observed. These reflections occur and disappear continuously. Figure 5 shows a time scan at the detector position of the CO<sub>2</sub> hydrate (321) Bragg reflection. The intensity strongly varies with time indicating fluctuations of the hydrate crystallites at the interface.

In order to investigate this hydrate formation more precisely, additional diffraction patterns were measured using the wide-angle diffraction setup with a MAR345 image plate detector at BL9 of the DELTA synchrotron source.<sup>32</sup> A slightly adapted sample cell with an inner diameter of 8 cm was used to investigate the hydrate formation in an interfacial area of about 80 mm<sup>2</sup>. This allows measuring the formation of crystallites at the interface with spatial resolution. After condensing a macroscopic thick liquid CO<sub>2</sub> film, Bragg reflections were immediately observable (see Figure 6). More scans after several minutes show a dynamic behavior of the formed hydrate clusters. The dynamics is still observable after about 100 min, and thus, no macroscopic freezing can be observed on this time

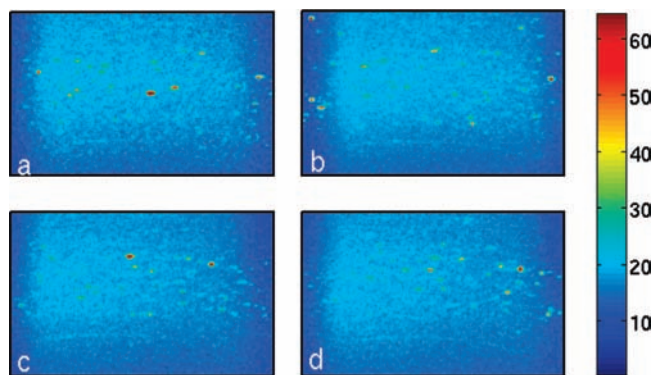


**Figure 6.** Diffraction images showing the region where the (321) reflection is observed. The intensity scale (arbitrary units) is presented right. (a) After filling with CO<sub>2</sub>. (b) After 60 min. (c) 95 min. (d) 97 min. A detailed representation of the time effects on the intensity of the (321) Bragg reflection is presented in Figure 5.

scale. By applying the Scherrer equation, a crystal size of approximately 200 Å can be estimated. Thus, the local formation of mobile hydrate crystallites which are moving freely at the interface was observed. A macroscopic formation, which would be observable by calorimetric measurements<sup>18</sup> or would show a freezing in of the dynamics at the surface, was not visible.

## Conclusion

Due to the instant formation of hydrate crystallites at the liquid–liquid interface, its stochastic nature, and the absence of any hydrate prestructures at the gas–liquid interface, the local structuring hypothesis is favored by our study. The formation on locally limited areas points to a rather stochastic process in contrast to the cluster models proposed by Sloan, Rodger, and Kvamme.<sup>1,2,9–11</sup> Hydrate layers or predicted prestructures which should appear at the water–gaseous CO<sub>2</sub> interface are not observable. The local formation of mobile CO<sub>2</sub> hydrate crystallites at the liquid–liquid interface and their size of approximately 200 Å suggests that the gas amount at the water–gas interface is too low for any hydrate formation, even in presence of an adsorbed CO<sub>2</sub> layer with a thickness up to 40 Å. Furthermore, these layers are disturbed by capillary wave fluctuations which may inhibit the formation of hydrates. Stable crystallites are formed in presence of a thick layer where the region of hydrate formation is less influenced by these fluctuations. Owing to the size of the crystallites which is about 1 order of magnitude above the expected nucleation size,<sup>8</sup> it can be deduced that an adsorbed layer with a thickness of at least 200 Å is necessary for hydrate formation at the water–gas interface.

## Summary

In summary, the water–gas interface shows in comparison to the liquid–liquid interface a very different behavior with respect to the gas hydrate formation process. The adsorption of gas molecules on the water surface leads to a high supply of CO<sub>2</sub> at the water surface but does not trigger the gas hydrate formation process. No hydrate formation could be observed for more than 8 h. In contrast we were able to observe formation of CO<sub>2</sub> hydrate at the water–liquid CO<sub>2</sub> interface. The presence of a macroscopic amount of liquid CO<sub>2</sub> induces the local formation of mobile CO<sub>2</sub> hydrate crystallites. Due to this finding, i.e. the stochastic nature of crystallite formation and the absence of surface covering prestructures at the interfaces, the local

(31) National Institute for Standards and Technology Chemistry WebBook; <http://webbook.nist.gov/chemistry>.

(32) Krywka, C.; Sternemann, C.; Paulus, M.; Javid, N.; Winter, R.; Al-Sawalih, A.; Yi, S.; Raabe, M.; Tolan, M. *J. Synchrotron Radiat.* **2007**, *14*, 244–251.

structuring hypothesis is selected as the adequate model for gas hydrate formation at the CO<sub>2</sub>–water interface.

**Acknowledgment.** We thank V. Honkimäki and S. Schröder for support, the ESRF and DELTA for providing synchrotron radiation, and the Bundesministerium für Bildung and Forschung

(BMBF Project Nos. 05KSPE1 and 05KSPEA) and the Deutsche Forschungsgemeinschaft (DFG Project No. TO 169/12-1) for financial support.

JA806211R